Role of Trialkoxysilane Functionalization in the Preparation of Organic-Inorganic Composites

Bradley K. Coltrain,* Christine J. T. Landry,* James M. O'Reilly, Alexandra M. Chamberlain, Gary A. Rakes, Joseph S. Sedita, Larry W. Kelts, Michael R. Landry, and Victoria K. Long

Research Laboratories, Eastman Kodak Company, Rochester, New York 14650-2116

Received April 7, 1993. Revised Manuscript Received July 19, 1993®

Organic-inorganic composite materials were prepared by in situ polymerization of tetraethoxysilane (TEOS) or tetramethoxysilane (TMOS) in the presence of both trialkoxysilane-functionalized and unfunctionalized poly(acrylates). The acrylic polymers were poly(methyl methacrylate) (PMMA), poly(methyl acrylate) (PMA), and poly(butyl methacrylate) (PBMA). Neutron activation, infrared spectroscopy, transmission and scanning electron microscopy, small-angle X-ray scattering (SAXS), dynamic mechanical, and stress-strain experiments were performed on these composites to determine the effect of trialkoxysilane functionalization. Slight differences in the local morphology were observed by SAXS; however, macroscopic phase separation was controlled to a large degree by the ability of the backbone to interact with the growing silicate network. Thus, PMMA and PMA composites were optically clear, but PBMA composites were opaque. Trialkoxysilane functionalization also aids in retarding phase separation and offers an increase in the glass transition temperature (T_g) with increasing silicate content, and a slight increase in the break stress. However, no differences in the tensile modulus, either below or above T_g, were observed between composites prepared from functionalized and unfunctionalized acrylates.

Introduction

A number of reports have appeared on the preparation of organic-inorganic composites (OIC) by in situ polymerization of metal alkoxides in organic polymers. These studies generally utilize organic polymers endcapped with trialkoxysilane moieties to facilitate cross-linking between the polymer and the growing inorganic oxide network.[1-20] Cross-reaction of the organic and inorganic components presumably retards gross phase separation, frequently producing homogeneous hybrid materials.

We[21-27] and others[28-35] have shown that it is possible to produce homogeneous, transparent OICs with highly dispersed inorganic oxide phases using organic polymers without trialkoxysilane functionality, if the polymer backbone structures are judiciously chosen. For example, transparent composites possessing high values for the rubbery plateau modulus above the polymer glass transition temperature (T_g) were obtained by reacting tetraethoxysilane (TEOS) under acid-catalyzed reaction conditions in solutions containing poly(vinyl acetate) (PVAc),[21,22] poly(methyl methacrylate) (PMMA),[23-25] and poly[bis((methoxyethoxy)ethoxy)phosphazene]

• Abstract published in *Advance ACS Abstracts*, September 1, 1993.

(1) (a) Schmidt, H.; Scholze, H.; Kaiser, A. *J. Non-Cryst. Solids* **1984**, *63*, 1. (b) Schmidt, H.; Kaiser, A.; Patzelt, H.; Scholze, H. *J. Phys. (Paris)* **1982**, *43*(C9), 275. (c) Philipp, G.; Schmidt, H. *J. Non-Cryst. Solids* **1984**, *63*, 283.

(2) (a) Mark, J. E.; Ning, Y.-P. *Polym. Bull.* **1984**, *12*, 413. (b) Mark, J. E. *Br. Polym. J.* **1985**, *17*, 144.

(3) (a) Mark, J. E.; Sur, G. S. *Polym. Bull.* **1985**, *14*, 325. (b) Mark, J. E.; Sun, C.-C. *Polym. Bull.* **1987**, *18*, 259.

(4) Pope, E. J. A.; Asami, M.; MacKenzie, J. D. *J. Mater. Res.* **1989**, *4*, 1018.

(5) Sur, G. S.; Mark, J. E. *Eur. Polym. J.* **1985**, *21*, 1051.

(6) Mark, J. E.; Wang, S.-B. *Polym. Bull.* **1988**, *20*, 443.

(7) Clarson, S. J.; Mark, J. E. *Polym. Commun.* **1987**, *28*, 249.

(8) Sun, C.-C.; Mark, J. E. *Polymer* **1989**, *30*, 104.

(9) Glaser, R. H.; Wilkes, G. L. *Polym. Bull.* **1988**, *19*, 51.

(10) Huang, H. H.; Orler, B.; Wilkes, G. L. *Macromolecules* **1987**, *20*, 1322.

(11) Huang, H. H.; Glaser, R. H.; Wilkes, G. L. *ACS Symp. Ser.* **1988**, *360*, 354.

(12) Glaser, R. H.; Wilkes, G. L. *Polym. Bull.* **1989**, *22*, 527.

(13) Glaser, R. H.; Wilkes, G. L. *J. Non-Cryst. Solids* **1989**, *113*, 73.

(14) Noell, J. L. W.; Wilkes, G. L.; Mohanty, D. K.; McGrath, J. E. *J. Appl. Polym. Sci.* **1990**, *40*, 1177.

(15) Rodrigues, D. E.; Brennan, A. B.; Betrabet, C.; Wang, B.; Wilkes, G. L. *Chem. Mater.* **1992**, *4*, 1437.

(16) Betrabet, C.; Wilkes, G. L. *Polym. Prepr.* **1992**, *33*, 286.

(17) Wei, Y.; Bakthavatchalam, R.; Whitecar, C. K. *Chem. Mater.* **1990**, *2*, 337.

(18) Kohjiya, S.; Ochiai, K.; Yamashita, S. *J. Non-Cryst. Solids* **1990**, *119*, 132.

(19) Coltrain, B. K.; O'Reilly, J. M.; Turner, S. R.; Sedita, J. S.; Smith, V. K.; Rakes, G. A.; Landry, M. R. In *Proceedings of Fifth Annual International Conference on Crosslinked Polymers*, Switzerland, 1991; p 11.

(20) Coltrain, B. K.; Rakes, G. A.; Smith, V. K. US Patent 5,019,607, 1991.

(21) (a) Fitzgerald, J. J.; Landry, C. J. T.; Pochan, J. M. *Macromolecules* **1992**, *25*, 3715. (b) Fitzgerald, J. J.; Landry, C. J. T.; Schillace, R. V.; Pochan, J. M. *Polym. Prepr.* **1991**, *32*(3), 532.

(22) Landry, C. J. T.; Coltrain, B. K.; Landry, M. R.; Fitzgerald, J. J.; Long, V. K. *Macromolecules* **1993**, *26*, 3702.

(23) Landry, C. J. T.; Coltrain, B. K.; Brady, B. K. *Polymer* **1992**, *33* (7), 1486.

(24) Landry, C. J. T.; Coltrain, B. K.; Wesson, J. A.; Lippert, J. L.; Zumbulyadis, N. *Polymer* **1992**, *33* (7), 1496.

(25) Landry, C. J. T.; Coltrain, B. K. US Patent 5,051,298, 1991.

(26) Coltrain, B. K.; Ferrar, W. T.; Landry, C. J. T.; Molaire, T. R.; Zumbulyadis, N. *Chem. Mater.* **1992**, *4*, 358.

(27) Coltrain, B. K.; Ferrar, W. T.; Landry, C. J. T. US Patent 5,010,128, 1991.

(28) Mauritz, K. A.; Warren, R. M. *Macromolecules* **1989**, *22*, 1730.

(29) Mauritz, K. A.; Storey, R. F.; Jones, C. K. *ACS Symp. Ser.* **1989**, *395*, 401.

(30) Mauritz, K. A.; Jones, C. K. *J. Appl. Polym. Sci.* **1990**, *40*, 1401.

(31) Davis, S. V.; Mauritz, K. A. *Polym. Prepr.* **1992**, *33* (2), 363.

(32) David, I. A.; Scherer, G. W. *Polym. Prepr.* **1991**, *32* (3), 530.

(33) Wung, C. J.; Pang, Y.; Prasad, P. N.; Karasz, F. *Polymer* **1992**, *32*, 605.

(34) Ravaine, D.; Seminel, A.; Charbouillot, Y.; Vincens, M. *J. Non-Cryst. Solids* **1986**, *82*, 210.

(35) Morikawa, A.; Iyoku, Y.; Kakimoto, M.; Imai, Y. *Polym. J.* **1992**, *21*, 107.

0897-4756/93/2805-1445$04.00/0

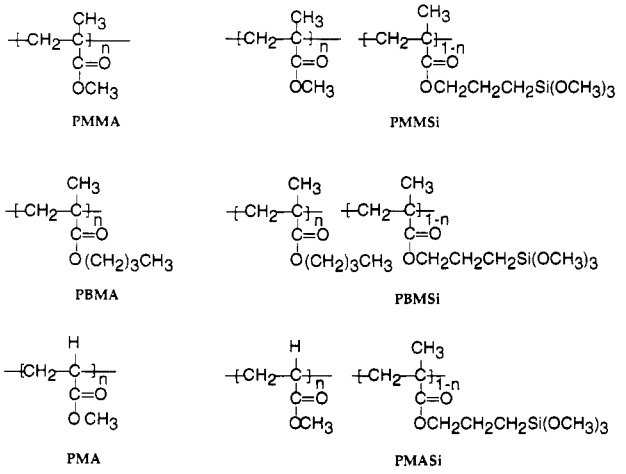

Figure 1. Polymer structures.

(MEEP).[26,27] In the PVAc and PMMA composites, extensive hydrogen bonding was present between the silanols of the silicate network and the carbonyl groups on the polymer. It is likely that hydrogen bonding also exists between silanols and ether oxygens on the MEEP side chains. This interaction between the polymers and the silicate network apparently retards phase separation.

Since homogeneous composites can be produced for polymers with or without trialkoxysilane functionality, a question arises as to what advantages are offered by the use of such functionalization in the generation of OICs. The trialkoxysilane functional groups are hydrolytically unstable, thus the polymers are subject to cross-linking upon exposure to moisture in the air. In addition, facile synthetic routes to trialkoxysilane-functionalized polymers do not always exist. Thus, it is desirable to determine if comparable composite properties could be obtained using nonfunctionalized polymers.

To compare the properties of functionalized versus nonfunctionalized OICs, it was necessary to select a suitable polymer system for study. One requirement is the use of a polymer capable of forming homogeneous composites both with and without functionalization. It would be desirable if the polymer was readily available or could be easily synthesized. Acrylic polymers met these criteria.

This paper describes the synthesis and characterization, the comparison of physical and mechanical properties, and the discussion of the morphological features of OIC materials generated from trialkoxysilane-functionalized and unfunctionalized acrylic polymers. During the course of this study it was found that no single polymer could be identified that was suitable for all comparisons, so three polymers were studied: PMMA, poly(butyl methacrylate) (PBMA), and poly(methyl acrylate) (PMA).

Experimental Section

The structures of the polymers used in this study are shown in Figure 1. Methyl methacrylate (MMA), butyl methacrylate (BMA), and methyl acrylate (MA) were obtained from Eastman Kodak Co. and were eluted on DHR-4 columns (Scientific Polymer Products) to remove inhibitors. [3-(Methacryloxy)-propyl]trimethoxysilane (MSi) was obtained from Aldrich and distilled prior to use. Tetrahydrofuran (THF) solvent was dried over sodium/benzophenone and distilled. Benzoyl peroxide was obtained from Aldrich and used as received. Azobisisobutyronitrile (AIBN) was obtained from Kodak and recrystallized from methanol prior to use. Tetraethoxysilane (TEOS, Fluka) and tetramethoxysilane (TMOS, Fluka) were used as received. PMMA was Plexiglas V(811)-100 from Rohm and Haas Co. having $\bar{M}_w$ = 79 000 and $\bar{M}_w/\bar{M}_n$ = 1.80 (in polystyrene equivalents) as determined by size exclusion chromatography (SEC) in THF.

Synthesis of [3-(Methacryloxy)propyl]trimethoxysilane-Functionalized Polymers. Poly(methyl methacrylate-*co*-[3-(methacryloxy)propyl]trimethoxysilane) (PMMSi), poly(methyl acrylate-*co*-[3-(methacryloxy)propyl]trimethoxysilane) (PMASi), and poly(butyl methacrylate-*co*-[3-(methacryloxy)propyl]trimethoxysilane) (PBMSi) were prepared by a modification of the procedure reported by Varma et al.[36] The polymers were prepared with <10 mol % MSi (typically 5%). At 10 mol % MSi or higher, the isolated polymer was frequently insoluble, presumably due to cross-linking of the silane moieties due to small amounts of moisture. At less than 10% MSi, cross-linking can easily be avoided as long as moisture is excluded from the reaction mixture and no heat is employed during vacuum drying. Heating during drying can lead to cross-linking, possibly due to loss of methyl ether from the silane groups.

The reactions were carried out with AIBN in THF at 60 °C under argon with stirring for 17–23 h. The polymers were isolated by precipitation from anhydrous methanol and dried in vacuo for 4 days. PMASi was precipitated from cold (−78 °C) anhydrous methanol due to the low T_g (T_g = 30 °C, from differential scanning calorimetry (DSC)). Typical yields of greater than 90% were obtained. The molecular weights were determined by SEC (in PS equivalents) to be $\bar{M}_w$ = 98 000 ($\bar{M}_w/\bar{M}_n$ = 2.6) for PMMSi, $\bar{M}_w$ = 87 000 ($\bar{M}_w/\bar{M}_n$ = 2.6) for PBMSi, and $\bar{M}_w$ = 40 000 (absolute) ($\bar{M}_w/\bar{M}_n$ = 2.7) for PMASi.

Synthesis of Poly(methyl acrylate) (PMA) and Poly(butyl methacrylate) (PBMA). These polymers were prepared and isolated as above. PMA was isolated from cold (−78 °C) anhydrous methanol due to the low T_g (T_g from DSC = 16 °C). The molecular weights were determined by SEC to be $\bar{M}_w$ = 41 000 (absolute) ($\bar{M}_w/\bar{M}_n$ = 2.7) for PMA and $\bar{M}_w$ = 298 000 (in PS equivalents) ($\bar{M}_w/\bar{M}_n$ = 2.2) for PBMA.

Preparation of Composites. Polymer solutions were prepared at 10, 15, or 20 wt % concentrations in THF (depending on the viscosity of the resulting solution). Silicon alkoxides were added on a mol % basis calculated on monomer molecular weight and molecular weight of a polymer repeat unit (100.12 g/mol for PMMA, 86.09 g/mol for PMA, and 142.18 g/mol for PBMA). The wt % SiO_2 can be calculated assuming full conversion of TEOS or TMOS. Hydrolysis of the silicon monomers was effected by addition of four molar equivalents of acidic water (0.15 M HCl, unless otherwise specified) based on the moles of Si. Composites with unfunctionalized polymers were prepared by stirring the polymer/TEOS solutions with the calculated amount of 0.15 M HCl for about 16 h at ambient temperature. The functionalized polymer/TEOS solutions were allowed to stir only 15 (PMMSi) or 30 min (PMASi and PBMSi) prior to casting or coating, due to rapid gelation. The composites were dried and cured at elevated temperatures in vacuo for several hours, as indicated in the text. The samples were stored in an N_2 atmosphere or in vacuo at room temperature until tested.

The above method of preparation will be referred to herein as using nonprehydrolyzed [nph] TEOS. Some composites were prepared with prehydrolyzed [ph] TEOS by first reacting 43 mL of TEOS, 20 mL of THF, and 14 mL of 0.15 M HCl in a closed vessel for 24 h at room temperature. The stock TEOS [ph] solution was then added to the polymer solution in the appropriate amount to give the desired wt % Si, mixed for 5 min, and cast.

PMMA and PMMSi composites were cast or knife-coated at ca. 30 °C, as described previously,[23,24] and air dried. These composites were extremely brittle, and samples were cut using a razor blade on 90 °C heated plates. The samples were then cured at 100 °C in vacuo for 20 h between glass plates.

The PMA and PMASi composites were cast into Teflon molds in a 50 °C oven and were covered to allow slow solvent evaporation and reduce bubbling and cracking. The composites were left in the oven for 48 h. Before cutting samples for mechanical property measurements, the films were dried in air from 60 to 100 °C over a period of a few hours. After cutting, the samples were cured in vacuo at 100 °C for 4 h and then 4 h at 130 °C.

The PBMA and PBMSi composites were cast into Teflon molds, however, the PBMA composite solutions were cast after only 30 min, as opposed to 16 h (as described for the PMA and

PMMA composites), and placed in a N_2-purged box for 5–7 days until dry. The dry castings were cured in vacuo to 100 °C over several days; at higher temperatures the polymer softened sufficiently to partially flow and distort the samples. The PBMSi samples could be cured to temperatures of at least 125 °C without difficulty. Samples for mechanical measurements were cut after curing.

A shorthand notation will be used to describe the composites. The molar percentage of added inorganic monomer will be noted as will the type and functionality of the organic polymer. For example, a composite with PMMSi-5 (containing 5% MSi) and 33 mol % TEOS will be denoted as PMMSi-5, 33% TEOS. (This composite contains 23 wt % SiO_2, assuming full condensation, although total conversion is unlikely at the low curing temperatures.)

Physical Property Measurements. ^1H NMR spectra were obtained on a General Electric Model QE-300 (300 MHz for protons) spectrometer using $CDCl_3$ as both internal standard and solvent. ^{29}Si NMR were obtained at 99.36 MHz on a Bruker AM-500 NMR spectrometer. Differential scanning calorimetry (DSC) measurements of T_g were made on a Perkin-Elmer DSC II using a heating rate of 20 °C/min. Dynamic mechanical (DMA) properties were measured using a Rheometrics Solid Analyzer (RSA-II). The driving frequency was 10 Hz and the temperature was typically scanned between −100 and 300 °C at a rate of 2–3 °C/min. Some of the samples, particularly the samples prepared with PMASi, were rather thick and taxed the limits of the RSA-II (instrument compliance). Thus, differences in the storage modulus, E', values in glassy regime should not be viewed as quantitative. However, values for moduli in the rubbery region above T_g are accurate. The percent silicon in cured samples was determined by neutron activation analysis (NAA). Fourier transform infrared (FTIR) transmission spectra of thin films cast onto KBr pellets were obtained using a Bio-Rad Digilab Division FTS-7 spectrometer (3240-SPC) with 4-cm^{-1} resolution.

Small-angle X-ray scattering (SAXS) measurements were performed on 0.2-mm-thick film specimens using an Anton Paar compact Kratky camera equipped with a Braun linear position sensitive detector. The reported SAXS profiles have been corrected for parasitic scattering and the contribution of background scattering of the organic polymer phase. The latter correction was done by subtracting the SAXS profile of the polymer, weighted by its volume fraction. Implicit in this procedure is the assumption that the filler phase does not affect the amorphous structure of the polymer. This was found to be a reasonable assumption for other OIC materials.[22] The scattering vector range recorded was q = 0.01–0.5 $Å^{-1}$, where $q = [(4\pi/\lambda)\sin(\theta/2)]$. λ (=1.54 Å) and θ are the X-ray wavelength and scattering angle, respectively. All profiles have been desmeared for the effects of slit collimation of the Kratky camera.[37] The SAXS data is presented in two forms. Intensity (or log I) versus q plots provide an idea of the scattering at all distance scales, and best show any maxima. Plots of log I versus log q emphasize the high-angle (or Porod law) region, which better emphasizes the local structure.

Transmission electron microscopy (TEM) was performed on samples that were sectioned with a Reichert Ultracut E. The samples were cooled during the sectioning with liquid nitrogen. The sections were ~80 nm in thickness and were transferred dry onto the TEM grids, dry pressed, and examined using a JEOL 100 CXII microscope at 100 kV. The intrinsic contrast between the organic polymer and the SiO_2 phase was sufficient such that no staining was required.

Ultimate mechanical properties were measured using a Sintech/20 testing machine equipped with a United environmental chamber (Model EUC3.5-600). Dogbone samples were machined from polymer films by rough cutting samples on the MK Model MG-125 DS diamond saw and machining to final test format on the TensilKut Model 10-88 router or by cutting them using an MS Instruments manual punch press and die. The die and lower platen were heated with a heat gun for those specimens that were too brittle to punch at room temperature. The sample geometry was a small dogbone specimen, and the crosshead speed was 2.5 mm/min (strain rate = 0.01 min^{-1}) following ASTM D638M-III. Engineering stress was calculated using the average cross-sectional area, and strain was calculated from the cross-head displacement using an effective gage length. Liquid nitrogen was used as the coolant in the environmental chamber for measurements made at subambient temperatures. Drierite was placed in the chamber to reduce moisture.

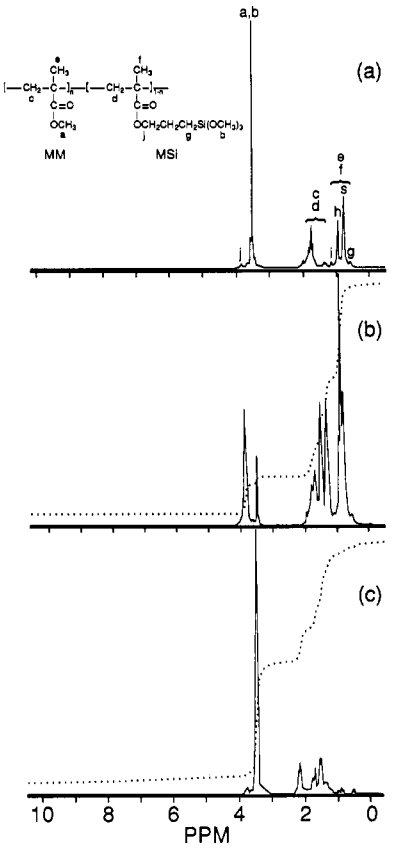

Figure 2. ^1H NMR spectra for (a) PMMSi-5, (b) PBMSi-5, and (c) PMASi-5. The symbols s, h, and i represent syndiotactic, heterotactic, and isotactic, as described in the text.

Results and Discussion

Chemistry. Acrylic polymers containing 1–10% MSi were readily synthesized. It is assumed that the MSi monomers are randomly distributed along the polymer chain in all cases, as Varma and co-workers[36] claimed for PMMSi. Overlapping signals in NMR spectra, particularly in PBMSi, make such verification difficult. Varma noted that the MSi concentration in the PMMSi copolymers tended to be slightly high relative to the monomer feed, indicating a slight preference of polymer radical for MSi. This was also observed in the present study, as indicated by neutron activation results.

Figure 2 shows ^1H NMR spectra for PMMSi-5, PBMSi-5, and PMASi-5, confirming the presence of MSi in the polymers. NMR spectra for the PMMSi copolymers were previously reported,[36] but some of the peaks were misidentified. Previously peaks at 1.89 and 1.0 ppm were identified as due to methyl protons and the peak at 0.8 ppm as due to the methylene protons α to Si.[36] The 1.89 ppm identification most likely represents a misprint, but the peaks at 0.8 ppm cannot be due to the methylene α to silicon as the integration is much too high. Integration

(36) Varma, I. K.; Tomar, A. K.; Anand, R. C. *J. Appl. Polym. Sci.* **1987**, *33*, 1377.
(37) Glatter, O. *J. Appl. Cryst.* **1974**, *7*, 147.

of the peaks at 1.7–1.9 ppm relative to the peaks at 0.8 and 1.0 ppm show a 2:3 ratio as expected for the methylene and methyl protons, respectively. The multiple resonances are probably due to polymer tacticity. Additional broad peaks are present at 1.3, 1.1, and 0.6 ppm. The peak at 0.6 ppm is likely due to the methylene α to silicon on the MSi monomer. The peak at 1.1 ppm is due to CH_3 protons of isotactic (i) PMMA, and the peaks at 1.0 and 0.8 ppm, to heterotactic (h) and syndiotactic (s) PMMA, respectively. The peak at 1.3 ppm is likely due to CH_2 repeat units of iso- and heterotactic PMMA. Integration of the 0.6 ppm peak indicates about 5.5 mol % MSi in the polymer (almost identical to the result of neutron activation), although only 5% was in the monomer feed.

The NMR spectrum for PBMSi (2b) was very similar to that for PMMSi. The primary differences are the presence of a new peak at 3.9 ppm due to OCH_2 protons and additional peaks between 1.0 and 1.5 ppm due to CH_2 resonances of the butyl groups. Integration of the peaks for PBMSi-5 gave a value of 4.2% MSi, whereas neutron activation results indicated almost exactly 5% incorporation. The spectrum for PMASi (2c) was similar, with the proton in the backbone of MA resonating as a broad peak at 2.0–2.3 ppm. Integration indicates incorporation of 5–6% MSi.

Homogeneous, transparent composites could be prepared with all of the polymers with the exception of PBMA. The original intent of this study was to focus upon PMMA and PMMSi composites as there was information already available on the PMMA composites.[23,24] However, these composites were too brittle to produce dogbone samples for measurement of ultimate mechanical properties (although morphology studies were successful). It was felt that the lower T_g of PBMA would allow the preparation of bulk samples. Large castings could be obtained with both PBMA and PBMSi series, but transparent PBMA composites could not be produced with TEOS or TMOS, even when the solution was allowed to mix for 16 h prior to casting, or was coated at elevated temperatures. Somewhat more homogeneous samples were produced with PBMSi. Apparently substitution of the methyl group by butyl increases the hydrophobicity enough to drive phase separation. If valid comparisons were to be made as to the effect of functionalization chemistry on the mechanical properties in the glassy state, we deemed it important to compare homogeneous samples. Work with MEEP and PMMA composites has shown that the mechanical properties are drastically different for homogeneous, transparent versus highly phase separated composites.[23,24,26] These results made it necessary to study PMA, as homogeneous composites could be prepared with both the functionalized and unfunctionalized polymers, and the low T_g allowed the production of bulk samples for mechanical property measurements.

One problem encountered with functionalized polymers is controlling the reaction rates of the alkoxysilane pendant group and the added silane monomer. Ideally, the added inorganic monomers should condense with the trialkoxysilane moieties on the polymer to enhance homogeneity. Unfortunately, this is a difficult reaction to monitor, particularly on a polymer. ^{29}Si NMR provides information about the degree of hydrolysis and condensation for the trialkoxysilane moieties as well as the tetraalkoxysilane monomer. However, it is difficult to determine whether the functionalized polymer condenses with itself or with

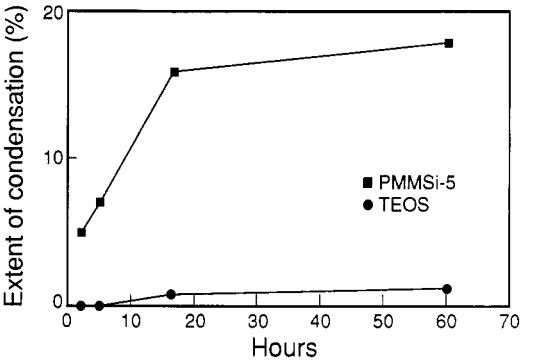

Figure 3. ^{29}Si NMR data comparing extent of condensation for TEOS and PMMSi-5.

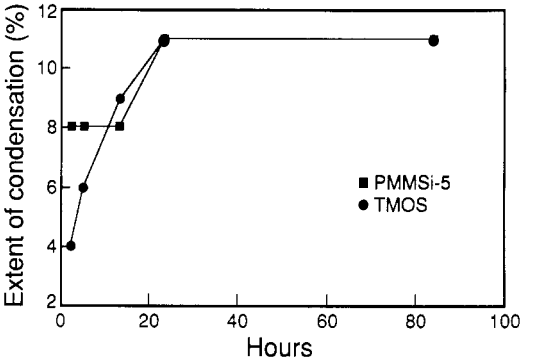

Figure 4. ^{29}Si NMR data comparing extent of condensation for TMOS and PMMSi-5.

added monomer, since ^{29}Si NMR is not very sensitive to nearest-neighbor effects in this system.

Figures 3 and 4 show ^{29}Si NMR data for the reaction of PMMSi-5 with TEOS and TMOS, respectively. In these plots the extent of condensation is plotted versus time. The extent of condensation is defined as the number of Si–O–Si bonds divided by the number of possible bonds assuming complete condensation. In these experiments only 1 mol of water, in the form of 0.15 M HCl, was added per mole of TMOS or TEOS. It is evident that the trimethoxysilane pendant groups react more rapidly than does TEOS but react at a similar rate to TMOS. This is supported by the fact that although a TEOS sol–gel mixture gels more slowly than does TMOS, the composite solutions of TEOS with PMMSi gel more rapidly (by approximately 20%). The polymer tends to react with itself first when TEOS is added (leading to rapid gelation), but the polymer can react with TMOS, retarding the polymer cross-linking. Alternatively, TMOS may be competing for the water present for the polymer cross-linking reaction. The spectra indicate a smaller percentage of the polymer has reacted when TMOS is added. It must be emphasized that these data do not prove that TMOS reacts with the polymer; it merely shows that reaction rates are more nearly matched with TMOS, suggesting that cross reactions may be more likely.

Analysis of the NMR data suggested that the TEOS composites may exhibit more microheterogeneity than the TMOS composites. However, as will be described later, no substantial differences were observed in the transparency of the films or in the DMA and SAXS results for PMMSi with TEOS versus TMOS. This implies that similar composite microstructures are formed using either monomeric precursor, and that the early stages of silicate condensation probed by the NMR experiment may play

only a minor role in microstructure formation, or that the properties are more dominated by the macrostructure that develops later.

It is likely that the trialkoxysilane groups eventually react with the silicate network formed from either TEOS or TMOS. It has previously been shown for trialkoxysilane encapped polystyrene that most of the condensation reactions between the pendant silane and the added monomer occur during drying and curing.[38] Thus, the fact that the methyl methacrylate backbone can interact with the silicate network and retard phase separation (as described previously[23,24]) may be the predominant factor dictating microstructural evolution. To obtain homogeneous coatings of the PMMA composites, slightly elevated coating temperatures were necessary as rapid vitrification retards phase separation.[23,24] In contrast, homogeneous castings of PMMSi composites were readily prepared at ambient temperatures, indicating an immediate difference due to functionalization. The trialkoxysilane moieties retard gross phase separation either by reacting with the inorganic oxide monomers or by rapidly gelling the system. It should be noted that these conclusions may not be valid for polymer backbones that cannot interact with the silicate network.

The percentages of Si in the composites, as determined by NAA, were generally close to the expected value, within ±2%. The notable exception to this was the PBMA, 50% TMOS composite that lost 85% of the added Si. This sample exhibited a greater degree of phase separation, and the SiO_2 preferentially migrated to one surface, as verified by scanning electron microscopy. Thus, the Si could be lost by the formation of a SiO_2 layer on one surface of the sample that could then "flake" away. These were generally opaque and highly phase separated.

Composite Morphology. Although elucidating the morphology was one of the goals of this study, the ultimate goal was to produce materials to be compared and contrasted with respect to mechanical properties. There were some unavoidable variations in sample preparation that could be reflected in the observed morphology. Thus, many of the morphology comparisons that follow were dictated by the requirements for mechanical testing.

The first comparison was with PMMA and PMMSi composites. The morphology of PMMA composites with TEOS was previously reported.[23] Highly dispersed SiO_2 phases with particle sizes on the order of 100 Å or less were observed by TEM for acid-catalyzed composites. However, TEM images of PMMSi with TEOS showed very little distinguishable structure. This characterization was augmented by SAXS. Scattering profiles are presented that sample the overall structure of the hybrids (I versus q), or that emphasize the local morphology (log I versus log q).

Figure 5 shows a direct comparison of SAXS profiles from knife-coated films of PMMA and PMMSi-5 containing 33 mol % of [ph] TEOS. The knife-coating format was chosen to compare the SAXS results with the mechanical properties measured previously by DMA.[23] TEOS was prehydrolyzed so that silicate polymerization could proceed for the same length of time in each of the composites (realizing that PMMSi gels very quickly, leaving little time for TEOS to polymerize if mixed directly). The SAXS profiles in Figure 5 show distinct

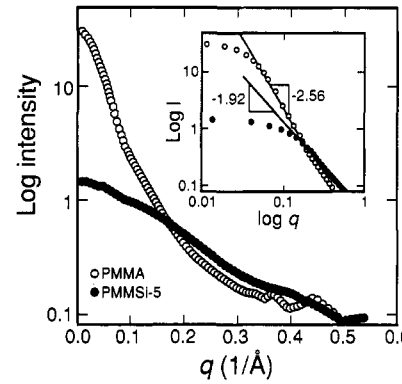

Figure 5. SAXS curves for knife-coated PMMA and PMMSi-5 films containing 33 mol % TEOS. The TEOS was [ph] before adding to PMMSi-5. A log–log plot is shown in the inset. (Oscillations in the PMMA profile are artifacts produced by the spline smoothing procedure used before desmearing the SAXS data.)

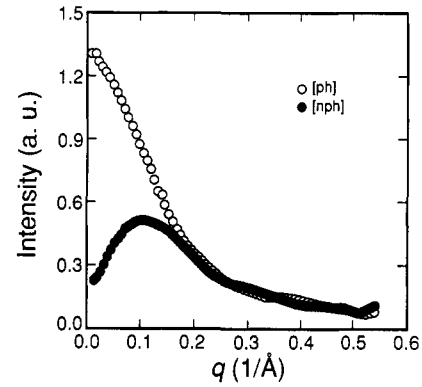

Figure 6. Comparison of desmeared SAXS profiles for [ph] and [nph] castings of PMMSi-5, 33 mol % TEOS composites.

differences between these samples, the most notable being the total scattered intensity. It is clear that the PMMA composite exhibits more scattering (both composites contain an identical (11 wt %) amount of Si, as determined by NAA). Examination of the Porod regions gives power-law slopes of −1.92 and −2.56 for the PMMSi and PMMA composites, respectively. The steeper slope indicates that the SiO_2 "network" is more dense in the PMMA composites, which also leads to higher scattering intensity. In other words, the unfunctionalized system exhibits a higher degree of phase separation or inorganic network consolidation. This observation suggests the functionalized polymer alters the inorganic phase reaction during drying. The fact that the power law exponents lie between −1 and −3 suggests that the inorganic phase is highly branched (mass fractal) rather than particulate (surface fractal, slope between −3 and −4).[39]

One of the variations in sample preparation of PMMSi-5 33% TEOS composites was solution casting followed by slow removal of the solvent, and knife coating, where evaporation was much faster. Another was using prehydrolyzed [ph] or nonprehydrolyzed [nph] TEOS. For [ph] TEOS, there are no notable differences in the SAXS profiles due to the casting procedure. However, a dramatic difference in the local morphology is seen when comparing castings from [ph] and [nph] TEOS with PMMSi-5 (Figure 6). The SAXS profile for the [nph] sample shows a scattering maximum. At smaller distance scales (larger

(38) Mourey, T. H.; Miller, S. M.; Wesson, J. A.; Long, T. E.; Kelts, L. W. *Macromolecules* **1992**, *25*, 45.

(39) Martin, J. E.; Hurd, A. J. *J. Appl. Cryst.* **1987**, *20*, 61.

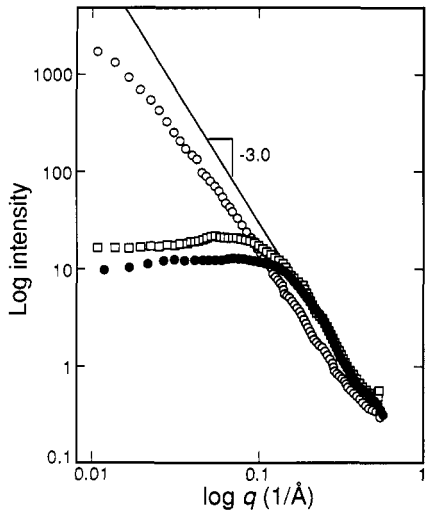

Figure 7. Desmeared SAXS profiles for (○) PMA, (□) PMASi-5 [ph], and (●) PMASi-5 [nph] composites with 20 mol % TEOS.

scattering angles) the profiles overlap, indicating that local structure for the two materials is similar. This will be discussed in more detail below.

Focusing now on the PMA system, no distinct phase separation is observed by TEM in the PMA and PMASi composites with TEOS, even at a magnification of 200000×. PMA composites exhibit essentially identical SAXS behavior to that observed with PMMA composites. The limiting slopes were −2.65 versus −2.56 for PMA/TEOS and PMMA/TEOS, respectively. However, the results for the PMASi composites were different. A comparison of [nph] versus [ph] is made in Figure 7 for PMASi-5 composites with 20 mol % TEOS. Also included in Figure 7 is the scattering curve for the unfunctionalized PMA composite. Contrary to the result seen for the PMMSi system, both PMASi profiles exhibit broad scattering maxima. The reason for the difference between [nph] and [ph] composites for PMASi vis-à-vis PMMSi is speculated as due to relative vitrification and phase separation rates between the two polymers. With T_g of PMASi being at approximately room temperature, enough mobility may be present for complete inorganic network formation and phase separation, whereas vitrification limits these in the PMMSi system. A possible mechanism for the morphology development will be described below. All three profiles indicate that the local inorganic network structures (<50 Å) are quite similar, as evidenced by the approach of the power law slope to −3. The steeper slope indicates a slightly denser inorganic phase in the PMA composites than for either PMMA or PMMSi samples. In fact, the behavior is similar to a fractally rough particulate. Again, the increase of the inorganic network density may partly be due to added mobility for network consolidation in the final heat processing step. It should also be noted that the PMASi composites were subjected to slightly higher processing temperatures (130 °C) than those with PMMSi (100 °C).

The presence of the broad scattering maximum was also seen in PMMSi-8 castings with either TEOS or TMOS, as shown in Figure 8, and at different loadings of the inorganic component, Figure 9. These were also made with [nph] alkoxides and can be compared with the results in Figure 6. The maxima are reminiscent of those observed with end-functionalized epoxy-based OICs[19] and several functionalized "ceramers" reported by the Wilkes group.[15]

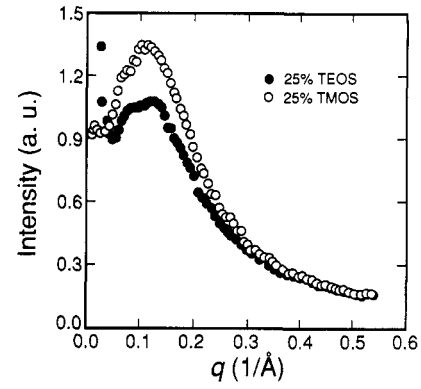

Figure 8. Desmeared SAXS profiles for PMMSi-8 with 25 mol % TEOS and TMOS castings. The correlation distance obtained by Bragg's law is 55 Å.

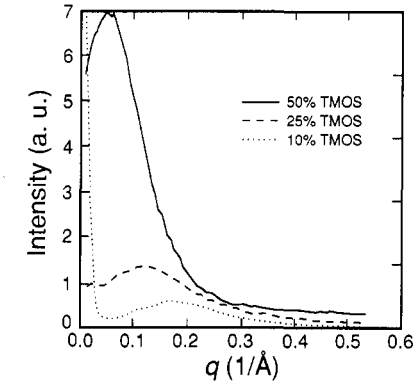

Figure 9. Scattering patterns for a TMOS concentration series with PMMSi-8 (castings). The peak positions represent correlation lengths of 33, 55, and 110 Å, respectively, for 10%, 25%, and 50% loadings.

Elucidation of the origin of the SAXS maximum in these materials was addressed in detail by the latter authors. A general morphological model was proposed that suggests the existence of a dispersed inorganic-rich phase attached at the interface of an organic-rich matrix phase through the functional sites on the organic polymer backbone. The position of the scattering maximum is a measure of the mean separation of the inorganic domains.

However, in a separate and more detailed modeling study[40] an alternate model is suggested that we believe more accurately describes the functionalized acrylate composites. The scattering maximum is thought to occur because of phase separation at local length scales by spinodal decomposition,[41] producing bicontinuous, interconnected structures. As the inorganic phase polymerizes in the solution stage, such as prior to casting and during slow solvent removal steps, there is a tendency for the organic and inorganic components to phase separate. Concomitantly, cross-linking of the functionalized polymer occurs, as well as some cross reaction between components. The inorganic phase is restricted to phase separating into open regions of the "mesh" produced by the cross-linked polymer. Unattached silicate clusters that invariably exist would also tend to diffuse into these regions and react. Varying the cross-link density leads to a different mesh size, which should cause a shift in the SAXS peak; this effect has been observed.[15] Particle growth in the polymer

(40) Landry, M. R.; Coltrain, B. K.; Landry, C. J. T.; O'Reilly, J. M., to be submitted to *Macromolecules*.
(41) Schaefer, D. W.; Mark, J. E.; McCarthy, D.; Jian, L.; Sun, C.-C.; Farago, B. *Mater. Res. Soc. Symp. Proc.* **1990**, *171*, 57.

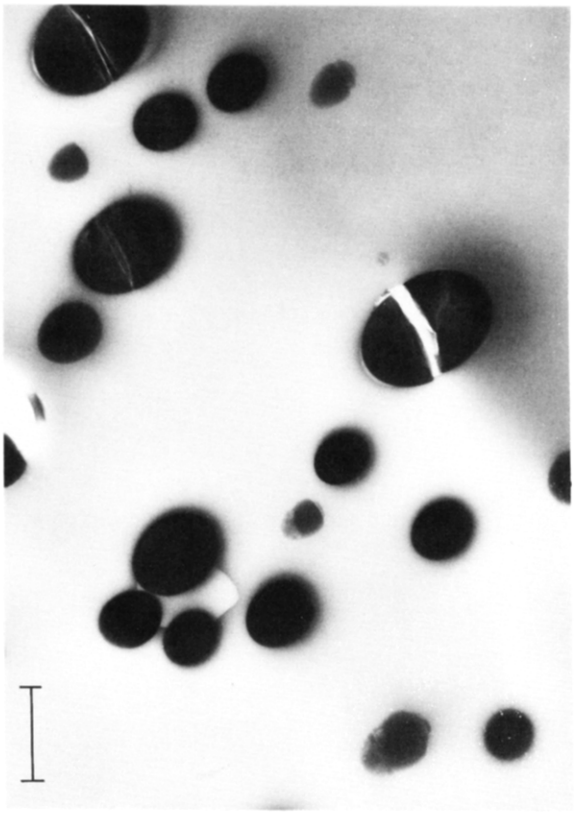

Figure 10. TEM of PBMA/25% TEOS with 0.15 M HCl. The fiducial bar represents a distance of 5.0 μm.

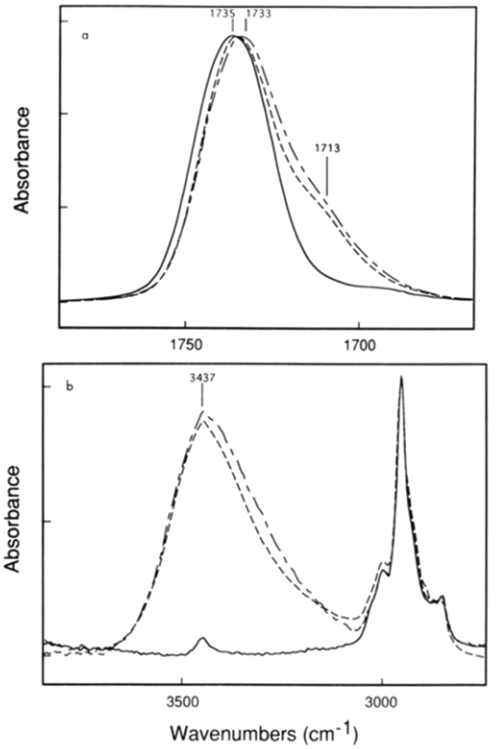

Figure 11. FTIR spectra of (a) the carbonyl and (b) the hydroxyl stretching regions for (—) PMA, (- - -) PMA/TEOS (26 mol %), and (– –) PMASi-5/TEOS [ph] (26 mol %).

mesh regions may lead to a similar picture as was suggested by Rodrigues and co-workers,[15] although with inorganic domains localized away from the polymer cross-link sites rather than at them.

The NMR results on the specific chemistries of TMOS and TEOS described earlier suggested a tendency for TEOS composites to be more phase separated than those with TMOS because of reactivity differences with respect to the MSi functional group. The total integrated intensity in TMOS samples was slightly higher for most of the PMMSi composites (Figure 8), indicating at size scales of about 500 Å and less there was a little more TMOS incorporated. An upturn at lower angles for TEOS composites was sometimes seen (Figure 8), implying the existence of larger particulates outside the resolution of the SAXS experiment. The final local structure for both the TEOS and TMOS composites was similar regardless of the details of the chemistry. This may in part be due to the mechanism of the final morphology formation, as well as partial compatibility of the methacrylate backbone with the silicate phase.

Last, characterization of the morphology of the PBMA composites is presented. In contrast to the PMMA and PMA composites, the PBMA samples showed macroscopic phase separation. TEM analysis of PBMA/25% TEOS revealed the presence of many large silicon oxide particles ranging from 2 to 8 μm in scale (Figure 10). SEM results on some composites (particularly those with TMOS) showed segregation of these particles towards one surface.

Composites prepared with PBMSi-5 were different for TEOS or TMOS. The [nph] polymerization of TEOS produced relatively translucent composites with 40–60-nm silicate-rich particles and occasional larger ones (100–200 nm). SAXS of this sample (not shown) exhibited a scattering maximum as seen for the other methacrylates, indicating that the local structure not visible by TEM (less than about 50 nm) was similar. In disparity with the TEOS materials, [nph] polymerization of TMOS produced opaque composites with micron- and submicron-sized particles. However, contrary to the grossly phase separated PBMA samples, the silicate particles appeared to be uniformly distributed rather than segregated to one side of the sample. Thus, the presence of the functional group MSi in systems having an inherent desire to phase separate appears to restrict the migration or settling out of the phase separated inorganic component.

It is apparent that MSi groups can be used to control phase separation to some degree. However, compatibility of the polymer backbone and the growing silicate network (or interactions between them) may be the overriding factor determining the final morphology.

Infrared Results. Figure 11 shows (a) the carbonyl and (b) the hydroxyl (OH) regions of infrared spectra of PMA [nph] and PMASi-5 [ph] composites with 26 mol % TEOS, compared to pure PMA. PMA has a strong absorption peak centered at 1735 cm^{-1} due to the carbonyl groups. A shoulder, centered at about 1713 cm^{-1}, appears in the composites' spectra. This shift to lower frequency is characteristic of hydrogen bonding to the carbonyl. The presence of residual silanols on the silicate network, which are capable of hydrogen bond formation, is evidenced in these composites by hydroxyl peaks in the 3100–3600-cm^{-1} region. The OH band is typically quite broad and is composed of several overlapping bands. Free hydroxyls would be reflected in a higher frequency band (ca. 3520–3600 cm^{-1}), whereas hydrogen-bound hydroxyls appear at lower frequencies. The shape and position of the maximum of the hydroxyl peaks for these composites are indicative of hydrogen bonding. Hydrogen bonding between silanols and the carbonyl oxygens of PMMA[24] or PVAc[21] has been well established. There appear to be

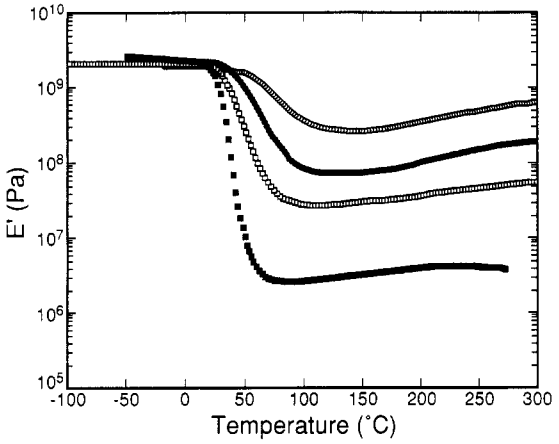

Figure 12. Temperature dependence of the storage modulus for PMASi-5/TEOS [nph] composites containing (■) 0, (□) 20, (●) 26, and (○) 38 mol % TEOS.

roughly comparable amounts of hydrogen-bound carbonyls in both PMA and PMASi composites. These results indicate that PMA and PMASi interact with SiO_2 networks produced from TEOS in a similar manner to that found for the PMMA composites. No evidence of hydrogen bonding was observed for the PBMA/TMOS composites. These data, taken together with the morphology results presented herein, suggest that hydrogen-bond interactions may play an integral part in controlling phase separation even in composites made from trialkoxysilane-functionalized polymers.

Mechanical Properties. The objective was to determine the effect of silane-functionalization on the mechanical properties of composites both in the glassy state and above T_g. DMA data for the PMA and PMASi composites are shown in Figures 12–14. Figure 12 shows the effect of adding TEOS to PMASi-5 on the temperature dependence of the tensile storage modulus (E'). The onset of the glass transition is accompanied by a drop in E'. Above T_g a rubberlike plateau in the storage modulus (E'_{pl}) is observed that extends to at least 300 °C and increases with SiO_2 content. Since PMASi itself is cross-linked, this plateau is evident even when no additional TEOS is added (in contrast to the nonfunctionalized systems[23]). Cross-linked polymers generally exhibit a plateau in E' above T_g, the magnitude of which is a function of the molecular weight between cross-links.[42] The PMA composites are compared with PMASi-5 (using both [ph] and [nph] TEOS) composites in Figures 13 and 14, each containing 26 mol % TEOS (20 wt % SiO_2) or 38 mol % TEOS (30 wt % SiO_2). The curves for [ph] and [nph] PMASi/TEOS composites are identical. Each system exhibits a rubberlike plateau in the storage modulus (E'_{pl}) above T_g. Although PMA itself does not exhibit a measurable E' above T_g, the magnitude of E'_{pl} for the PMA/TEOS composite is the same as for a PMASi/TEOS composite with the same SiO_2 content. A broad relaxation peak is observed in tan δ at the T_g. A gradual increase in the onset and breadth of T_g is also observed with increasing SiO_2 content for the PMASi composites. Similar, although not identical, results are observed for the PMA/TEOS composites. The onset of the α transition is somewhat sharper and occurs at a slightly lower temperature, and the shape of the tan δ peak is different. Although for the

(42) Ferry, J. D. *Viscoelastic Properties of Polymers*, 3rd ed.; John Wiley: New York, 1980; Chapter 14.

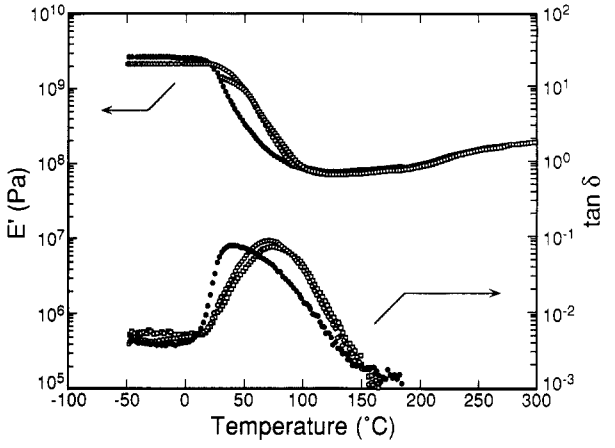

Figure 13. Temperature dependence of the storage modulus and tan δ for composites containing 26 mol % TEOS: (●) PMA/TEOS, (○) PMASi-5/TEOS [nph], and (□) PMASi-5/TEOS [ph].

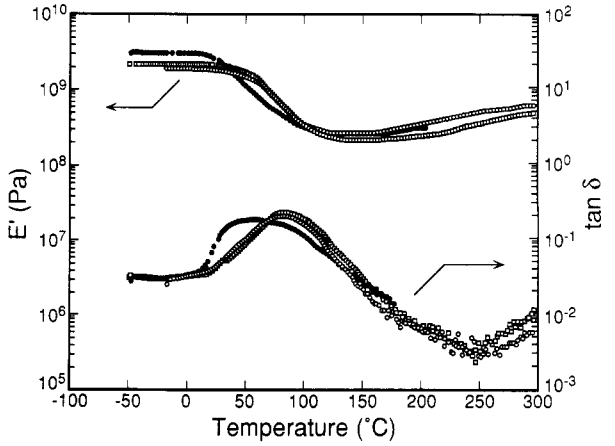

Figure 14. Temperature dependence of the storage modulus and tan δ for composites containing 38 mol % TEOS: (●) PMA/TEOS, (□) PMASi-5/TEOS [nph], and (○) PMASi-5/TEOS [ph].

Table I. DMA Results for PMMSi-8 Composites[a]

sample	tan δ (max), (°C)	E'_{pl} (MPa)
PMMSi-8	126	20
PMMSi-8, 10% TMOS	140	20
PMMSi-8, 10% TEOS	128	~10 (broke)
PMMSi-8, 25% TMOS	134	~70 (broke)
PMMSi-8, 25% TEOS	136	80
PMMSi-8, 50% TMOS	151	>500 (broke)
PMMSi-8, 50% TEOS	165	400
PMMSi-5, 33% TEOS [ph][b]	140	200
PMMA, 33% TEOS[b]	100	80

[a] All solutions were [nph], except as noted. [b] Knife coatings.

SiO_2 loadings studied herein the onset of T_g in the nonfunctionalized systems does not shift much with increasing SiO_2 content, the transition broadens substantially.

DMA data for the PMMA and PMMSi composites are summarized in Table I. Knife coatings of PMMA and PMMSi-5 with 33 mol % TEOS were prepared; the PMMA sample was coated at ca. 30 °C and the PMMSi sample at room temperature. The DMA results for this direct comparison are shown in Figure 15. The increase in T_g for the functionalized samples is clearly observed. The PMMSi composite shows a slightly higher plateau modulus, although at higher temperatures the differences in the rubbery plateau are substantially reduced. E'_{pl} for these composites increases substantially with temperature during the DMA experiment, as was previously observed

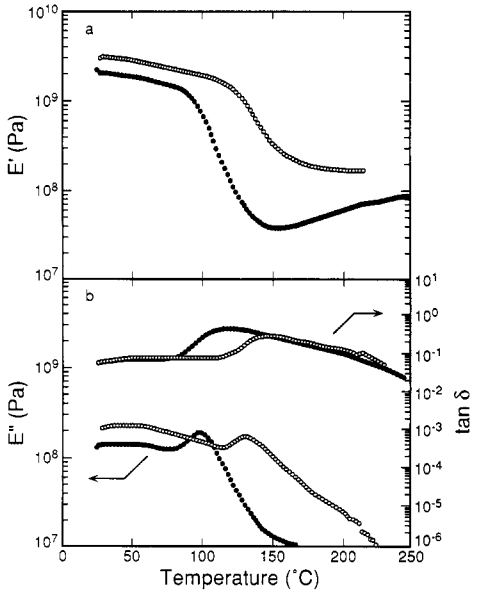

Figure 15. DMA spectra (a) (E') and (b) E'' and tan δ, for knife coatings of (●) PMMA and (○) PMMSi-5 with 33 mol % TEOS.

in a number of OIC systems.[21-23,26] This is presumed to be due to loss of residual solvent and/or further cross-linking of the silicate network upon heating. This effect can be reduced by curing the composite above T_g (as was done for the PMA samples) and seems to be less pronounced in the functionalized systems. The tan δ curves are substantially broadened by the addition of TEOS for both samples, and are quite similar in shape. It is also enlightening to compare the results for PMMSi composites with those previously reported for PMMA composites.[23,24] The plateau modulus for 53 mol % TEOS composite with PMMA reported previously[23] (cured in vacuo at 90 °C for 63 h) is about 10^8 Pa, which is slightly lower than that reported here for PMMSi-8, 50 mol % TEOS (4×10^8 Pa). In general, adding increasing amounts of TEOS or TMOS to PMMSi results in substantial broadening of the tan δ peak, an increase in T_g, and an increase in E'_{pl}.

The data discussed to this point demonstrate that the PMMA and PMMSi composites behave in a similar dynamic mechanical manner to those of PMA and PMASi, despite some differences in the silicate network structure (SAXS). Unfortunately, to compare mechanical property data in the glassy region for PMA and PMASi composites it was necessary to employ subambient temperatures, because the T_g's of the PMA composites are near ambient temperature. The samples were initially tested at 0 °C but proved to be quite brittle, making it difficult to make the measurements. Therefore, the remaining samples were tested at 8 °C. Unfortunately, it was not possible to make a direct comparison of ultimate properties of the PMA and PMASi composites at this higher temperature (8 °C) as the modulus of the PMA composites dropped due to the vicinity of the T_g.

Mechanical properties of PMA and PMASi-5 composites are summarized in Table II. Although it is necessary to make some comparisons at two different temperatures (0 and 8 °C), it is felt that the differences in these temperatures are small enough to permit carefully drawing some conclusions. Due to difficulties in obtaining this data, attention should be focused on general trends rather than specific, subtle differences.

Analysis of both the PMA and PMASi composites measured at 0 °C demonstrates that the tensile modulus

Table II. Mechanical Properties of PMA and PMASi Composites[a]

sample	T (°C)	modulus (MPa)	break stress (MPa)	break strain (%)
PMA/TEOS				
20% [nph]	0	2031(163)	29(3)	1.8(0.3)
26% [nph]	0	2579(546)	30(7)	1.1(0.3)
38% [nph]	0	2899		
PMASi-5/TEOS				
20% [nph]	0	2337(402)		
26% [ph]	0	2899(252)	53(19)	1.9(0.6)
26% [nph]	0	3327(119)	54(6)	1.7(0.2)
PMA/TEOS				
26% [nph]	8	1795(276)		
PMASi-5/TEOS				
26% [ph]	8	2780(337)	66(7)	3.0(0.4)
26% [nph]	8	2542(262)	58(8)	2.8(0.5)
38% [ph]	8	2771(449)	36(12)	1.4(0.4)
38% [nph]	8	2699(221)	36(14)	1.4(0.5)

[a] The numbers in parentheses indicate the standard deviation.

increases with increasing SiO_2 loading, as has been previously observed with similar systems.[21] At 8 °C this trend is not evident. The modulus value for PMA/TEOS at 8 °C is quite low due to proximity to the T_g of the polymer phase for this composite. Comparing results at 0 °C, the effect of polymer functionalization can be observed. The modulus results (and breaking stress results for the 26 mol % TEOS [nph] samples) for 20 mol % TEOS loadings are statistically higher. However, it is important to note that the T_g values for PMA and PMASi are different (PMASi-5 = 30 °C and PMA = 16 °C from DSC). It should also be remembered that the DMA results showed the addition of TEOS to PMASi-5 results in a substantial increase in T_g, whereas its addition to PMA results in only a slight T_g increase. Thus, the more appropriate choices for data comparison are the results at 0 °C for PMA and at 8 °C for PMASi-5 composites, as these measurements are made at more similar ΔT values below T_g.

Comparing the results for both the 26 and 38 mol % TEOS composites, there is no statistical difference between modulus values for the PMA and PMASi composites. However, both the breaking stress and strain are higher for the latter (in the case of the 26% sample). Thus, only modest differences in mechanical properties exist between PMA ansd PMASi composites. Although the data are scattered and some questions remain, it is felt that large differences in mechanical properties would have been detected. The dominant effect of the presence of MSi groups is an increase in T_g of the composite.

Although the butyl methacrylate composites were phase separated, the mechanical property results were enlightening. Table III lists the mechanical properties of the PBMA composites. A few trends are evident. Focusing first on the data for the PBMA series, note that T_g (tan δ peak maximum) did not change as Si was added, consistent with the PMMA and PMA results. Also note that no measurable plateau in the modulus above T_g was observed for any of the composites. This is in contrast to the results for PMA, PMMA,[23,24] MEEP,[26] and PVAc,[21] which all showed high plateau moduli upon the addition of TEOS. Undoubtedly this difference is due to the fact that the composites with PBMA were highly phase separated.

Turning now to the PBMSi series (Table IIIb), note that T_g was found to increase with increased loading of Si and when acidic water was added to the blank. As expected

Table III

sample	cure temp (°C)	tan δ (max) (°C)	E'_{pl} DMA (MPa)	modulus (MPa)	break stress (MPa)	break strain (%)	yield stress (MPa)	yield strain (%)
(a) Mechanical Properties of PBMA Composites[a,b]								
PBMA (blank)	100	58	none	290(19)	11(0.2)	219(30)	11(0.2)	7(0.2)
PBMA (blank, repeat)	100	65	none	243(24)	9(0.2)	214(9)	9(0.2)	8(0.7)
25% TMOS	100	58	none	262(57)	9(0.3)	140(14)	9(0.7)	8(1.7)
25% TMOS (1 M HCl)	100	65	none	291(42)	9(0.4)	201(14)	9(0.4)	8(1.1)
50% TMOS	100		none	255(30)	7(1)	140(62)	10(0.4)	8(0.6)
25% TEOS	100	65	none					
PBMA (blank)	125		none	262	11	173	11	7
25% TMOS	125		none	252	9	25	9	7
(b) Mechanical Properties of PBMSi Composites[a,b]								
PBMSi-5 (no water)	100	60	none	161(29)	7(0.03)	222(14)	7(0.2)	12(1.1)
PBMSI-5 (0.15 M HCl)	100	70	2.0	201(12)	10(0.04)	25(10)	10(0.4)	10(0.8)
25% TMOS (1 M HCl)	100	88	4.3					
50% TMOS	100	90	18.0					
PBMSi-5	125	56	none	183(25)	9(0.6)	211(15)	8(0.3)	11(1.1)
25% TMOS	125	75	4.5	724(33)	21(0.6)	22(2)	20(0.2)	5(0.2)
25% TEOS	125	84	7.0	646(24)	21(0.9)	16(11)	21(0.9)	5(0.7)

[a] The numbers is parentheses indicate the standard deviation. [b] All solutions were [nph].

for these polymers, a plateau occurs in the storage modulus above the T_g of the PBMSi, which increases with increasing SiO_2 content. None was detected for the blank until water was added, indicating that atmospheric moisture was not effective in facilitating the hydrolysis and condensation reactions of the MSi groups.

Samples of both PBMA and PBMSi with 25 mol % TMOS were prepared using 0.15 M HCl and 1 M HCl as catalysts. It was felt that 1 M HCl might increase the hydrolysis and condensation rates of the added monomer and provide a better match of reaction rates with the MSi moieties. It is well-known that $Si(OR)_4$ species react more slowly than $R'Si(OR)_3$ (for $R' = CH_3$) species under acid conditions.[43] Thus, a more efficient cross reaction between the polymer and the growing silicate network might be anticipated, which could lead to better homogeneity and hence better mechanical properties. Slightly better properties were obtained for both the PBMSi and PBMA composites with 1 M HCl as the catalyst.

The fact that the PBMSi-5/TEOS composite was visibly more homogeneous likely explains why the TEOS composite shows a higher T_g and plateau modulus than the TMOS sample at the same Si loading. Also, the slight inhomogeneity seen in the PBMSi-5/25% TEOS sample may contribute to a substantially lower plateau modulus than one would predict based on the PMMSi-8/25% TEOS.

Young's modulus was found to increase sharply with increasing Si addition. In fact, the samples rapidly became so brittle that stress–strain analysis could not be obtained, and thus there are gaps in the data in Table IIIb. Break and yield stress were found to increase with SiO_2 loading although strain at break decreased slightly. It should be noted that the most valid comparisons are with the blank with added water since this sample had clearly cross-linked. Unfortunately, the high degree of phase separation in the PBMA samples precluded further mechanical property studies of these composites.

Summary

Composites were prepared by in situ polymerization of TEOS or TMOS in the presence of trialkoxysilane-functionalized or unfunctionalized acrylic polymers in order to determine the effects of silane functionality on physical properties and morphology. The polymers functionalized with MSi were found to gel very rapidly. This limitation was at least partially overcome by prehydrolyzing the TEOS prior to addition. Homogeneous composites were obtained for PMMA and PMA systems. However, the substitution of methyl by butyl on methacrylate polymers (PBMA versus PMMA) had a pronounced effect on the phase separation behavior in the composites. Hydrogen bonding between the silicate and the polymer was observed in the PMMA and PMA composites but not in the PBMA composites. The addition of MSi moieties along the chain improved the homogeneity of the composites somewhat. This was illustrated by optical clarity, SEM, and TEM on the PBMSi relative to the PBMA composites.

Whereas a plateau in the tensile modulus above T_g (E'_{pl}) was observed only with highly homogeneous OIC composites prepared from unfunctionalized polymers (MEEP, PMMA, PMA, PVAc), a functionalized polymer such as PBMSi cross-links, and a rubbery plateau in the modulus was observed even when the system was phase separated. Plateau moduli were found to increase with increasing addition of TEOS for the PMMA and PMA composites, but no plateau in the modulus above T_g was detected for the PBMA composites, due to the high level of phase separation in the latter. Thus, PMMSi, PMASi, and PBMSi composites all showed E'_{pl} values that increased with the addition of TEOS or TMOS, regardless of whether or not the composite was phase separated. However, greater reinforcement was observed for the more homogeneous materials. The homogeneous PMMSi/25% TEOS had a higher plateau modulus than did the more phase separated PBMSi/25% TEOS sample. TEOS composites of PBMSi were more homogeneous than the corresponding TMOS composites, which translated into an improved plateau modulus for PBMSi/TEOS versus PBMSi/TMOS.

In the case of homogeneous composites with MSi functionality, T_g values were found to steadily increase with increasing amount of silicate. This was in contrast to the results on unfunctionalized PMMA or PMA in which the onset of T_g was found to be virtually independent of TEOS loading, at least for the loadings studied herein.

SAXS indicated that there was little discernible difference in microscopic morphology of the inorganic

(43) Brinker, C. J. J. Non-Cryst. Solids 1988, 100, 31.

network between castings or knife coatings, but a substantial difference was noted for PMMSi composites when the TEOS was [ph] versus [nph] prior to its addition. A broad SAXS peak was observed for the latter [nph], but was absent in the former [ph]. However, this difference ([ph] versus [nph]) was not observed for the PMASi composites. This is likely a reflection of differences in vitrification behavior due to the different T_g's of the PMA and PMMA systems during microphase separation.

The brittle nature of many of the samples at large volume fractions of the polymer implies that the inorganic and organic phases are co-continuous. The presence of reactive sites along the organic polymer backbone appears to lead to a more intimate mixture of the two phases, as evidenced by the more tenuous, or low-density, nature of the inorganic network. Cross-linking of the polymer chains, which may partially lead to the observed increase in T_g, also appears to limit the silicate phase separation. NMR results on PMMSi indicated that TEOS reacts more slowly than the MSi groups, whereas TMOS reactivity more nearly matched that of the pendant silanes. This suggested that the TMOS samples could be more homogeneous, but no large differences were observed by SAXS. At present, the belief is that a bicontinuous interpenetrating network-like structure is formed by spinodal decomposition or a similar mechanism for the samples exhibiting SAXS maxima. A better description of the structures will require study during their formation.

In general, very little difference was observed in mechanical properties for any of the PBMA composites relative to the blank, whereas the Young's modulus, break stress, and yield stress were found to increase in the PBMSi composites with increasing silicate content. Yield strain and break strain decreased for the PBMSi composites. This illustrates the effect that compositional changes along the polymer backbone can have on phase separation, and the effect that phase separation can have on mechanical properties. No significant differences were observed in the mechanical properties of PMA versus PMASi composites, particularly for the modulus, both above and below T_g. A slightly higher breaking stress was obtained with composites of functionalized polymers.

The conclusions indicate that it may be possible to optimize certain mechanical properties, such as break stress and T_g, using trialkoxysilane-functionalization. The primary effect of MSi functionalization on mechanical properties was an increase in T_g with increasing amount of silicate. Equally important was the fact that comparable moduli (in both the glassy and rubbery states) can be obtained with silicate composites prepared from unfunctionalized polymers. The ability to achieve comparable properties with unfunctionalized materials means that the storage problems associated with the use of hydrolytically unstable functionalized polymers can be avoided. Additionally, specialty synthesis of functionalized polymers is not required. Interactions between the polymer backbone and the growing inorganic oxide network were found to be important, and may play a more dominant role in determining composite morphology than does alkoxysilane-functionalization.

Acknowledgment. We thank B. V. Sorenson, J. M. Salva, and S. R. Turner for technical assistance and R. O. Gutierrez, D. Schwark, and R. G. Bowen for their invaluable contributions in microscopy.